FOURTEENTH EUROPEAN ROTORCRAFT FORUM

Paper No. 44

AIR RESONANCE STABILITY OF HINGELESS ROTORS IN FORWARD FLIGHT

James M. Wang, Jinseok Jang and Inderjit Chopra

Center for Rotorcraft Education and Research
Department of Aerospace Engineering
University of Maryland
College Park, Maryland 20742, U.S.A.

20-23 September, 1988
MILANO, ITALY

ASSOCIAZIONE INDUSTRIE AEROSPAZIALI
ASSOCIAZIONE ITALIANA DI AERONAUTICA ED ASTRONAUTICA

Air Resonance Stability of Hingeless Rotors in Forward Flight[1]

James M. Wang[2], Jinseok Jang[3], and Inderjit Chopra[4]

Center for Rotorcraft Education and Research
Department of Aerospace Engineering
University of Maryland
College Park, MD 20742, U.S.A.

1 ABSTRACT

Air resonance in forward flight is examined for hingeless rotors using a finite element formulation. The fuselage is modeled as a rigid body undergoing five degrees of freedom. The trim and blade response solutions are calculated as one coupled solution using a modified Newton method. The blade response is calculated using a finite element method in time after the nonlinear finite element equation in space are transformed to normal mode equations. Unsteady aerodynamic effects are also included using dynamic inflow modeling. The linearized periodic coupled rotor-body perturbation equations in the nonrotating frame are solved for the stability roots using Floquet transition matrix theory as well as constant coefficient approximation. Systematic parametric studies are then carried out to examine the effects of several design variables on air resonance stability in forward flight. Blade stiffness and fuselage roll inertia were found to have powerful influence on air resonance stability.

2 INTRODUCTION

Since the 1960's there has been considerable interest in hingeless rotors because of mechanical simplicity, better maintainability, and increased control power. To achieve manageable bending stresses and vibrations, hingeless rotors are usually designed as soft-inplane rotors. However, soft-inplane rotors may be susceptible to rotor-body aeromechanical instabilities known as ground resonance and air resonance. Ground resonance is caused by the coupling of low frequency lag mode with

[1]presented at the 14th European Rotorcraft Forum, Milano, Italy, September 20-23, 1988
[2]Research Assistant
[3]Research Associate
[4]Professor

landing gear modes. Air resonance occurs on an airborne vehicle and is caused by the interaction of the low frequency lag mode with the coupled flap and airframe modes. For articulated rotors, the aeromechanical instability problems are solved by adding blade lag dampers. Because of the lack of a lag hinge, lag dampers can not be used effectively. Thus, there is a need to determine precisely the aeromechanical stability of hingeless rotors in order to avoid air resonance instability at different flight conditions.

The coupled rotor-body aeromechanical stability of hingeless rotors has been examined by a number of researchers [1-14]. In reference [4,5], authors examined ground and air resonance in hover for a hingeless rotor using a simplified structural modeling for the blade (rigid blade with offset hinge). They also carried out some limited correlation of predicted air resonance stability boundary with measured data from a BO-105 model rotor. They showed that soft-inplane hingeless rotor can be designed to be free from unstable aeromechanical behavior by correct placement of blade and body frequencies, and judicious choice of hub design parameters. In Reference [6], authors analyzed air resonance stability of a hingeless rotor in hover and forward flight using a time history solution technique. It concluded that air resonance is sensitive to control stiffness, collective pitch and precone. Ormiston [7] made a systematic study of the fundamental characteristics of ground and air resonance of hingeless rotors in hover using a simple rigid blade analysis. It was shown that rotor flapwise stiffness can significantly influence hingeless rotor-body aeromechanical stability. King [8] conducted air resonance analysis and correlation with a model Lynx rotor, but it was limited to hovering flight. Because of the complexity in forward flight aeromechanical stability analysis, most of these studies are confined to hover air resonance analysis. There is a need for forward flight air resonance stability study, and to identify the effects of various design parameters on forward flight air resonance. There is also a need for improved structural and aerodynamic modeling.

Recently, it has been shown that the inclusion of a dynamic inflow model to account for the influence of unsteady aerodynamic effects improves the prediction of aeromechanical instability. In Reference [9], Peter addressed the sensitivity of helicopter aeromechanical stability to dynamic inflow in hover. Johnson [10] calculated the modal frequencies and dampings for a hingeless rotor on a gimballed support in hover and compared the results with measured data. Good correlations were obtained when the dynamic inflow model was used. Also an inflow mode was identified and correlated with measured data. Later on Friedmann and Venkatesan [11] analyzed the influence of dynamic inflow models on the aeromechanical stability of a hingeless rotor in ground resonance for the same rotor configuration as examined in Reference [10]. Again, it was shown that adding dynamic inflow improves the prediction of aeromechanical instability.

Most of the existing studies on air resonance stability use a simple structural

modeling for the blade (rigid blade with an equivalent hinge representation), quasisteady aerodynamics, and are confined to hovering flight. In the present paper, forward flight air resonance stability is investigated using a refined structural modeling for the blade (elastic blade undergoing flap bending, lag bending and elastic twist), dynamic inflow modeling, and coupled trim. A systematic parametric study was carried out to examine various design parameters on forward flight aeromechanical stability. The present analysis is based on the bearingless rotor stability analysis covered in Reference [14,15,16].

3 ANALYSIS

The air resonance stability analysis of a hingeless rotor in forward flight consists of two phases: calculating coupled vehicle trim and rotor steady response, and then calculating stability perturbations of rotor-body equations of motion. From the coupled trim analysis, control settings, vehicle attitude, blade steady response and hub loads are determined. Then, using Floquet theory, the stability roots of the rotor-body problem are obtained.

The rotor dynamic analysis is based on finite element method in space, and time. Each blade is assumed as an elastic beam undergoing flap bending, lead-lag bending, elastic twist, and axial deflections. The blade is discretized into a number of beam elements. Each element has fifteen degrees of freedom. Between elements there is continuity of displacement and slope for flap and lead-lag deflections, and a continuity of displacement for axial displacement and geometric twist. There are two internal nodes for axial displacement, and one for twist. The model assumes a cubic variation in flap bending, lag bending, and axial displacements, and a quadratic variation for twist [14,24].

To analyze blades with swept tip, it is assumed that the geometric angle at the interface, between unswept and swept portions of blade, is preserved before and after deformation. In the assembly of two adjoining elements at the interface, the compatibilities for displacement, velocity and acceleration terms are satisfied. Also, the effect of sweep is introduced in the derivation for elemental inertial characteristics of the blade. [20]

Quasi-steady strip theory is used to obtain the aerodynamic loads. Noncirculatory forces based on thin airfoil theory are also included. Unsteady aerodynamics effects are introduced approximately through a dynamic induced inflow modeling. For this, Pitt and Peters [19] model is used.

3.1 Coupled Vehicle trim and Rotor Steady Response

Coupled trim analysis in forward flight consists of vehicle trim (propulsive), blade steady response and hub loads calculation. The trim solution is calculated from the overall nonlinear vehicle equilibrium equations: three force equations (longitudinal, lateral and vertical) and two moment equations (pitch and roll). The yawing moment equilibrium equation is not included because the yawing angle is considered to have negligible influence on rotor response and stability solution. For a specific advance ratio μ and thrust coefficient, the propulsive trim solution determines pilot control settings $(\theta_{75}, \theta_{1c}, \theta_{1s})$ and vehicle attitude (α_s, ϕ_s).

The blade steady response solution involves the determination of time dependent blade deflection at different azimuth positions. This steady response solution is calculated using a finite element in time which is formulated from the Hamilton principle in the weak form [21]. Third order Lagrangian shape functions in time are used within each time element. The blade steady response equations are nonlinear periodic equations. For the response solution, the time period of one rotor revolution is discretized into a number of time element, and then the periodicity of response is imposed on the assembling of finite element equations. To reduce computation time, these equations are transformed to the normal mode domain using the coupled natural vibrational modes of the blade. Then, the steady response is calculated from a few nonlinear algebraic normal mode equations.

Then the hub loads are obtained by the force summation method. The blade inertia loads and the motion-induced aerodynamic forces are integrated along the span to obtain the blade loads at the root, and then summed over all the blades to obtain the rotor hub loads.

For a coupled trim solution, the propulsive trim solution based on rigid flap dynamic is used as an initial guess for the first iteration. For the subsequent iterations, the vehicle trim and the rotor response are calculated as one coupled solution using a modified Newton method. It is noted that the overall vehicle forces and moments equilibrium equations are always satisfied by a converged coupled trim solution [23].

3.2 Stability Solution

For the stability analysis, the blade perturbation equations of motions are obtained by linearizing the blade equations about its steady deflected position. To

reduce computation time, the resulting perturbation equations of motion are transformed into the normal mode domain using the coupled free vibration characteristics of the blade about the the mean deflected position. The blade normal mode equations in the rotating frame are then transformed to the nonrotating frame using multiblade coordinate transformations. For air resonance in hover, only the cyclic modes in the blade motions are considered. For air resonance in forward flight, the collective and the reactionless modes in addition to cyclic modes are considered, since these also influence the coupling terms.

For hover air resonance analysis, the perturbation rotor, body and inflow equations in the nonrotating frame contain constant coefficients. Therefore, the equations are solved as an algebraic eigenvalue problem. For forward flight studies, the perturbation rotor, body and inflow equations in the nonrotating frame contain periodic terms and these are solved for stability roots using Floquet transition matrix theory. To help identify the proper frequency and damping for a particular mode, the constant coefficient approximation approach is used.

4 RESULTS AND DISCUSSION

4.1 Correlation with Ground Resonance Results

To check the theoretical formulation, ground resonance calculations in hover were correlated with Reference [12] configuration 1 experimental data. Both quasisteady aerodynamics, and dynamic inflow modeling results were compared with experimental data. It is found that including dynamic inflow modeling gives better correlation to the experimental data. The results are presented in Figures 1 - 7.

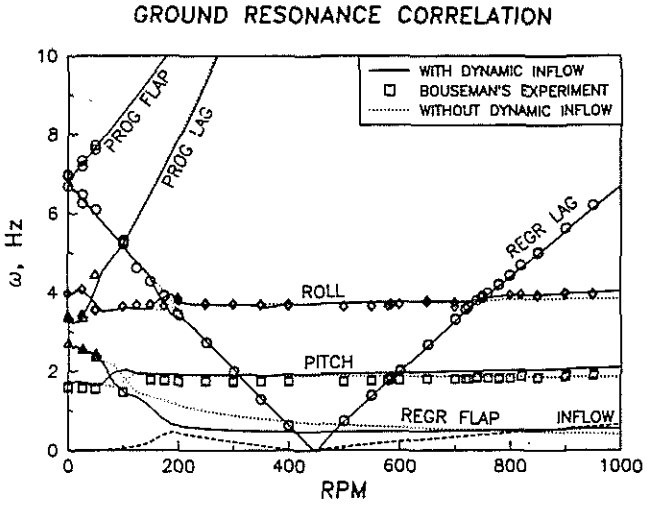

FIG. 1 MODAL FREQUENCIES FOR CONFIGURATION 1. $\theta = 0^\circ$

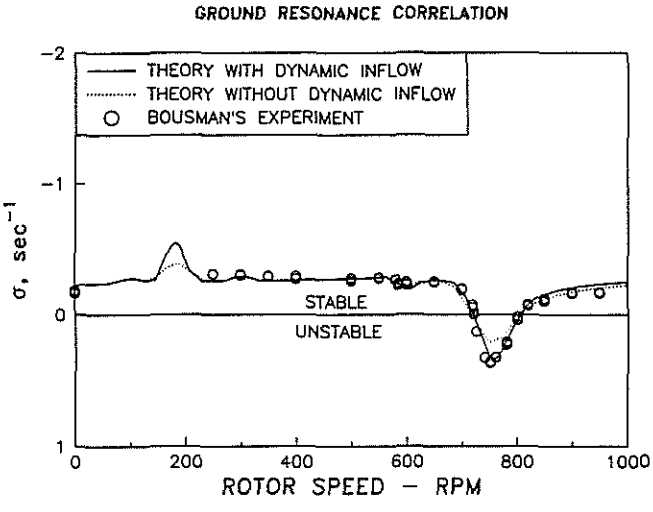

FIG. 2 REGRESSING LAG MODE DAMPING VS RPM FOR CONFIGURATION 1 $\theta = 0^\circ$

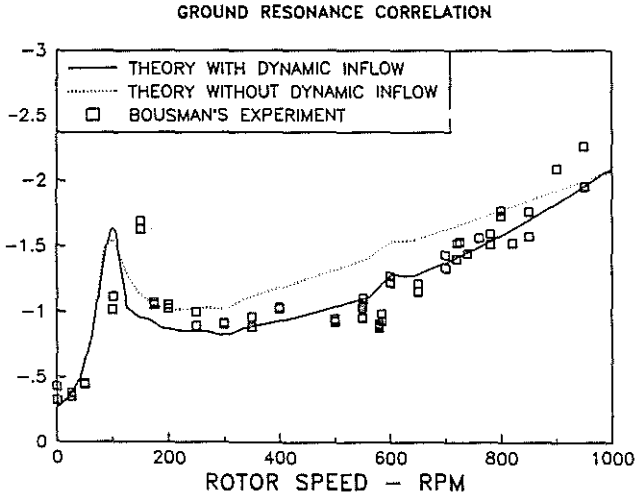

FIG. 3 BODY PITCH MODE DAMPING VS RPM FOR CONFIGURATION 1 $\theta = 0^{\circ}$

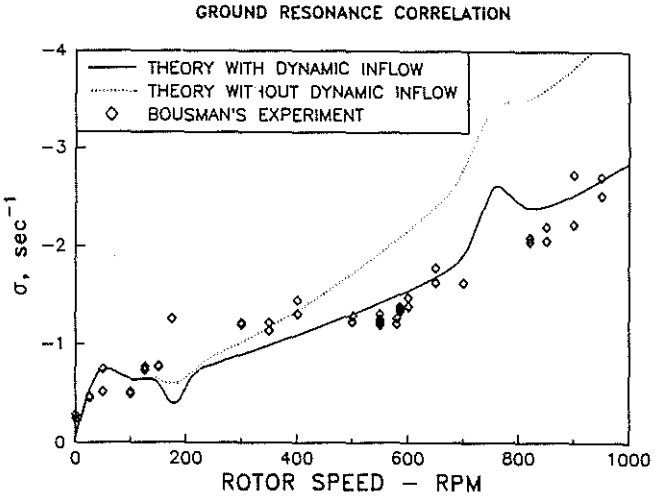

FIG. 4 BODY ROLL MODE DAMPING VS RPM FOR CONFIGURATION 1 $\theta = 0^{\circ}$

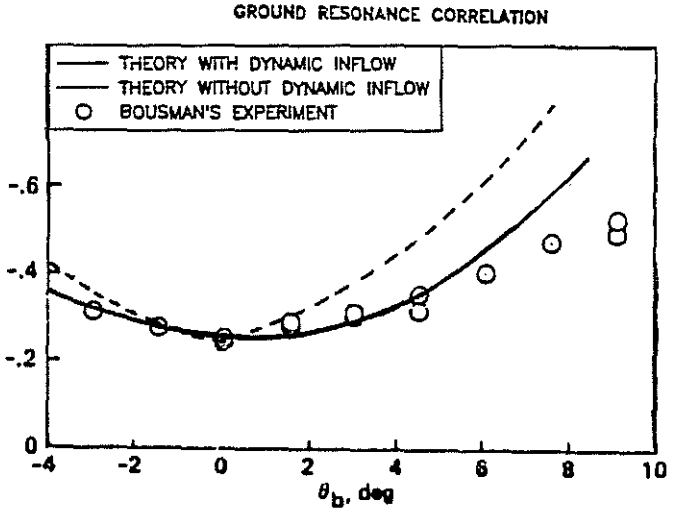

FIG. 5 REGRESSING LAG MODE DAMPING AS A FUNCTION OF BLADE PITCH ANGLE FOR CONFIGURATION 1 AT 650 RPM.

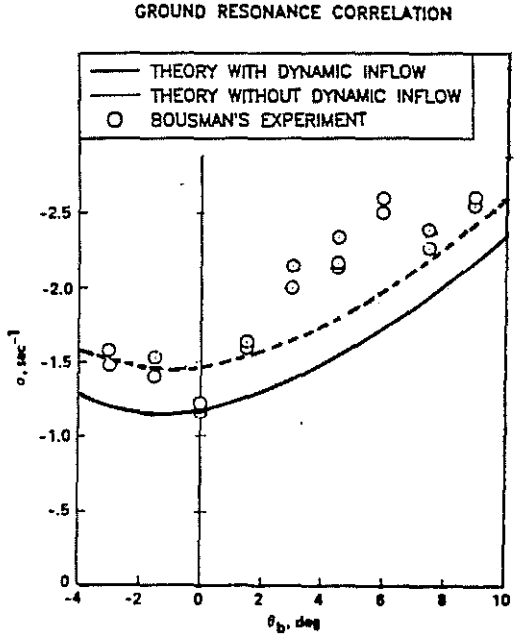

FIG. 6 BODY PITCH MODE DAMPING AS A FUNCTION OF BLADE PITCH ANGLE FOR CONFIGURATION 1 AT 650 RPM.

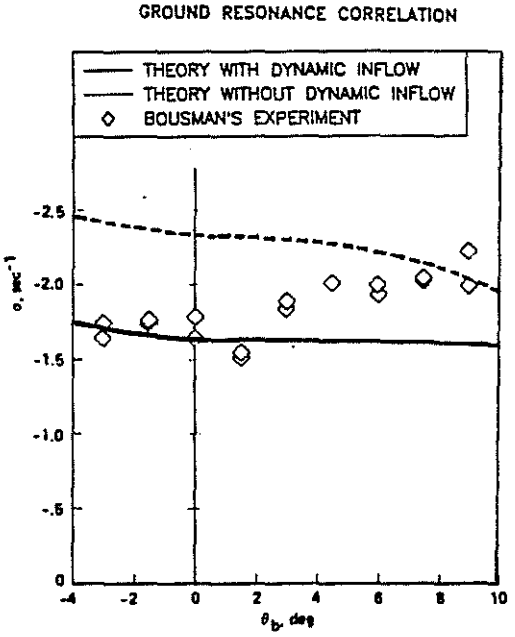

FIG. 7 BODY ROLL MODE DAMPING AS A FUNCTION OF BLADE PITCH ANGLE FOR CONFIGURATION 1 AT 650 RPM.

4.2 Effect of Number of Body Modes on Hover Air Resonance

For Hover and forward flight analysis, a typical 4 bladed hingeless rotor is used. The blade properties and the body data used are given respectively in Table 1 and Table 2.

Table 1 Hingeless Blade Structural Properties

Element	Flapwise $\frac{EI_y}{m_0\Omega^2R^4}$	Chordwise $\frac{EI_z}{m_0\Omega^2R^4}$	Torsion $\frac{GJ}{m_0\Omega^2R^4}$	Mass $\frac{m}{m_0}$	Radius of Gyration $\frac{k_m}{R}$	Length $\frac{\ell}{R}$
1	.01080	.02680	.00615	1.0	.029	.15
$2-6$	.01080	.02680	.00615	1.0	.029	.17

Table 2 Rotor and Fuselage Data

Number of Blades, N_b	4
Chord/Radius, c/R	.055
Lock Number, γ	5.5
Solidity Ratio, σ	.07
Hub Vertical Offset, h/R	.2
Lift Curve Slope, a	5.73 /rad
Lift Coeff., c_ℓ	$.15 + 5.73\ \alpha$
Drag Coeff., c_d	$.0079 + 1.7\ \alpha^2$
Pitching Moment Coeff., $c_{m_{ac}}$	-.012
Blade Linear Twist, θ_{TW}	0°
Precone, β_p	0°
Sweepback, Λ	0°
Roll Inertia, I_x/m_0R^3	2.7395
Pitch Inertia, I_y/m_0R^3	7.4331

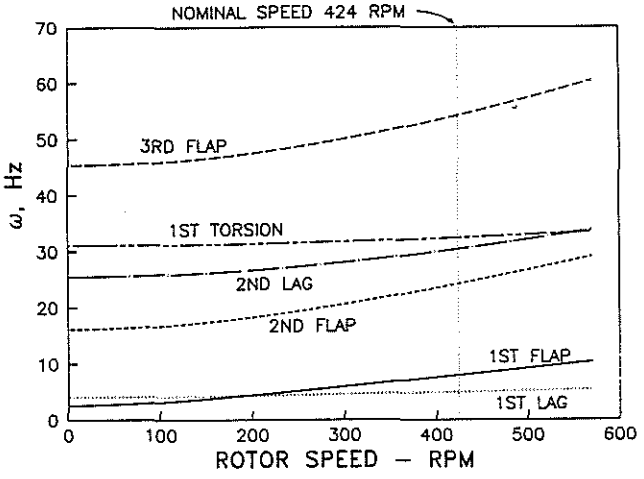

FIG. 8 FAN DIAGRAM OF FREQUENCIES VERSUS ROTOR SPEED

For hover calculations, the blade is discretized into six elements. For the stability solution, six coupled rotating normal modes are used (3 flap, 2 lag, 1 torsion). The fan diagram of frequencies versus rotor speed at zero collective pitch is shown in Figure 8. The nominal operating speed for this rotor is chosen to be 424 rpm. At this rotor speed, the rotating fundamental natural frequencies of the blade are: flap frequency = 1.13/rev, lag frequency = 0.70/rev, and torsion frequency = 4.58/rev, which represent a typical soft-inplane rotor. Inherent structural dampings for all the blade and body modes are neglected. For hover, the collective and differential collective modes do not couple with body modes and therefore are neglected. The total number of states depend on the number of body modes: 24 states due to the rotor (6 modes. progressing and regressing), 2 states due to inflow ($\lambda_{1c}, \lambda_{1s}$), and 2 states for each body mode used.

For the hover stability solution, the effects of body modes are presented in Figures 9 through 15. the shaft fixed results are compared with when five body modes are used (pitch, roll, and 3 translations). The stability results are presented in terms of decrement ratio.

$$DECREMENT\ RATIO = -\frac{\sigma}{\Omega_{ref}}$$

Decrement ratio is defined as the real part of the complex eigenvalue with a negative sign, and divided by the reference rotor speed. A positive value of decrement ratio represents stable condition, while negative value represents instability.

Results for two different collective pitch settings are shown. Comparing Figure 9 and Figure 10, it is clear that for either 0° or 8°, the progressing flap and lag frequency results are quite identical whether body modes are neglected or when five body modes are used. However, the low frequency regressive flap and inflow modes results are influenced by the addition of body modes.

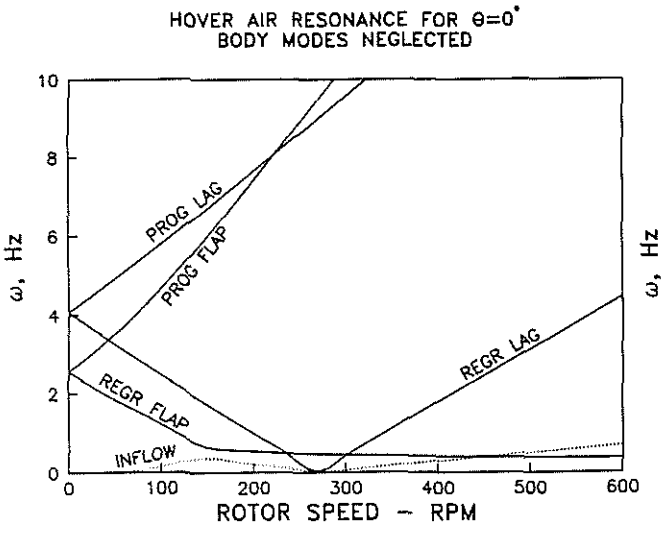

FIG. 9a MODAL FREQUENCIES FOR AIR RESONANCE

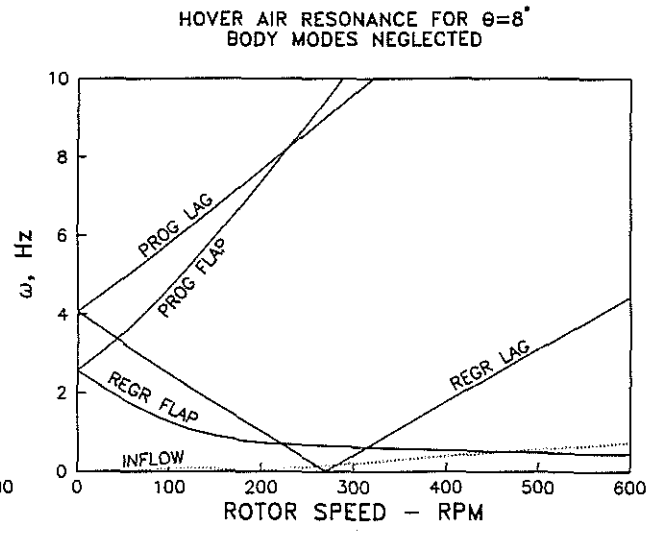

FIG. 9b MODAL FREQUENCIES FOR AIR RESONANCE

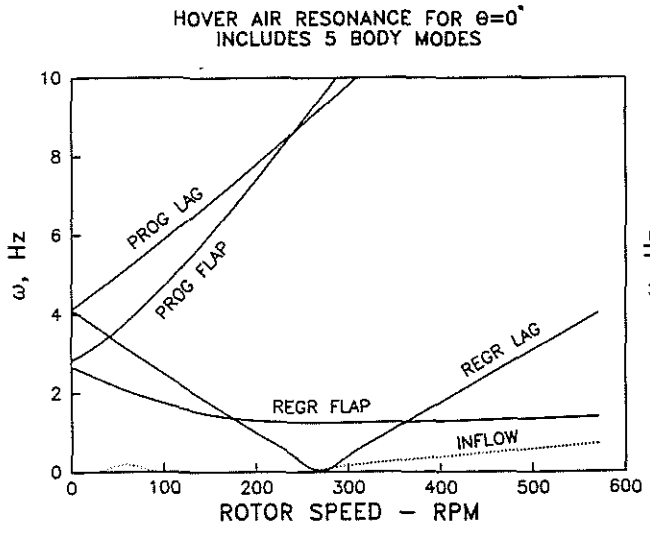

FIG. 10a MODAL FREQUENCIES FOR AIR RESONANCE

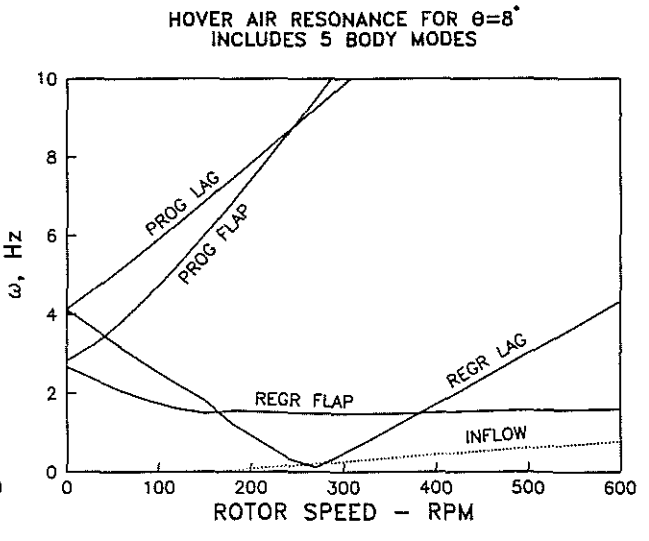

FIG. 10b MODAL FREQUENCIES FOR AIR RESONANCE

Figure 11a and 12a present the flap modes and inflow mode dampings for 0° collective pitch. Neglecting the body modes has minimal effects on damping of flap modes and inflow mode at high rotor speeds. But at low rotor speeds, the damping results are different for two cases. At 8° collective pitch, neglecting the body modes has only small effect on the flap and inflow modes damping. These results are presented in Figure 11b and 12b.

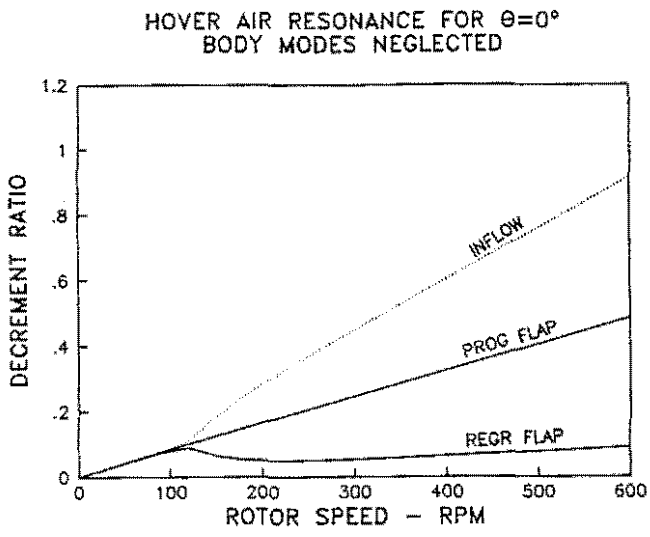

FIG. 11a FLAP AND INFLOW MODES DAMPING

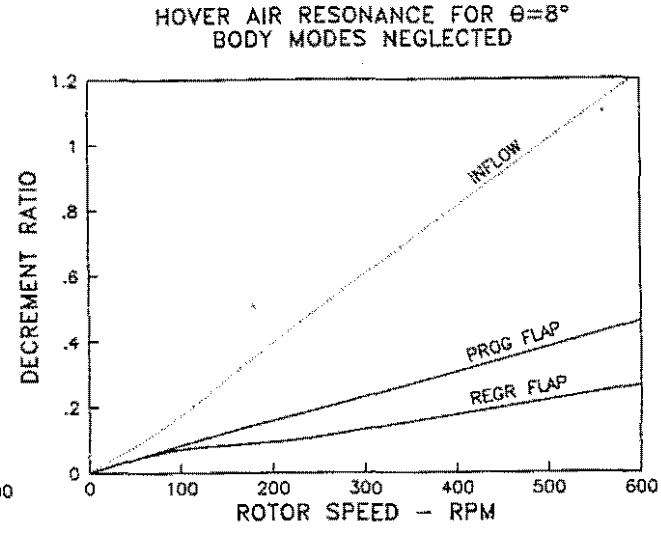

FIG. 11b FLAP AND INFLOW MODES DAMPING

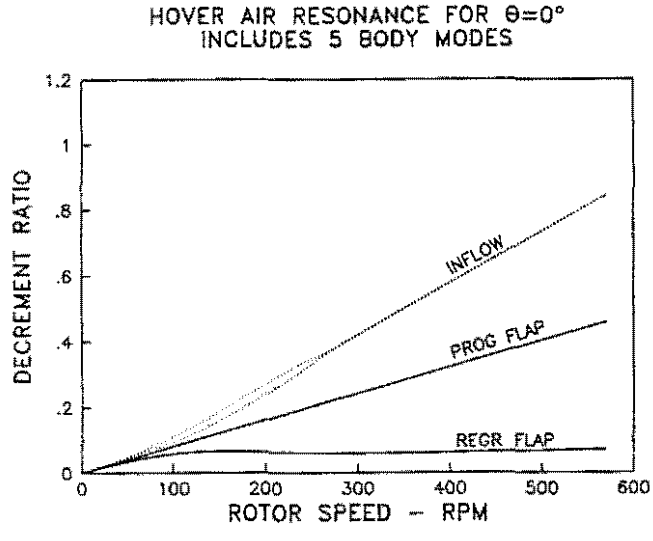

FIG. 12a FLAP AND INFLOW MODES DAMPING

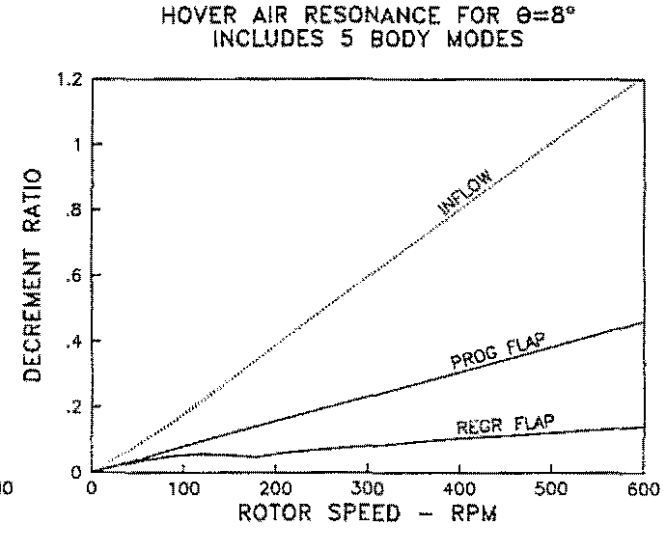

FIG. 12b FLAP AND INFLOW MODES DAMPING

It is known that ground resonance is caused by the coupling of the low frequency flap and lag modes with the body modes. Thus, if the body modes are neglected, then the rotor-body aeromechanical instability problem would not be predicted properly. Figure 13 and 14 show that the lag modes damping results are strongly affected by the body degrees of freedom.

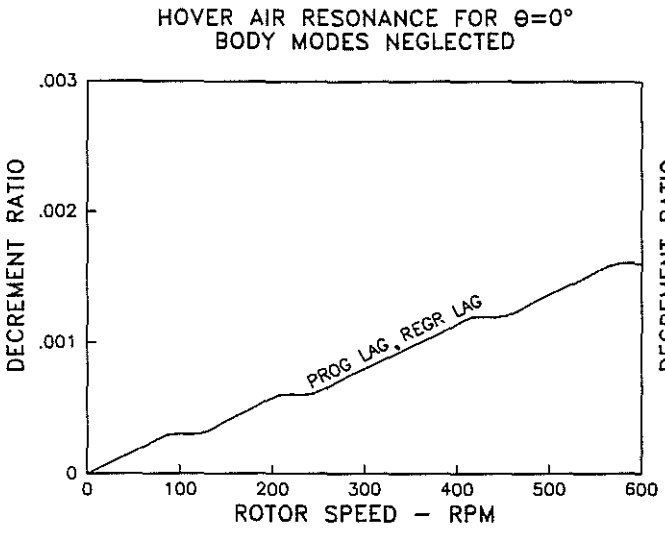

FIG. 13a LAG MODES DAMPING

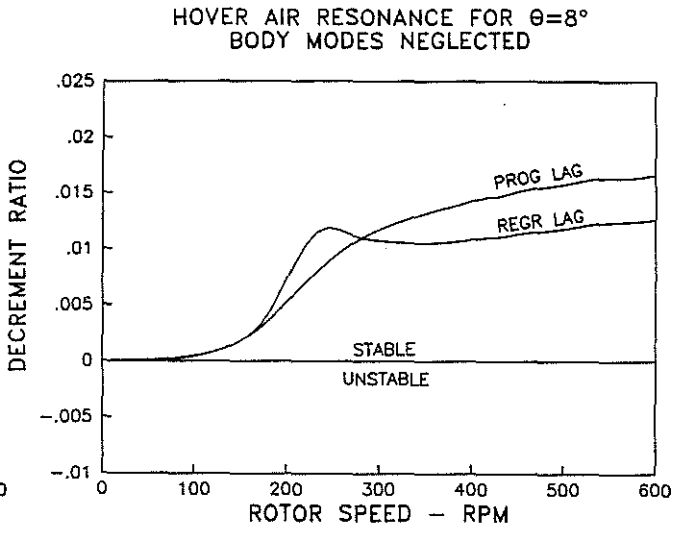

FIG. 13b LAG MODES DAMPING

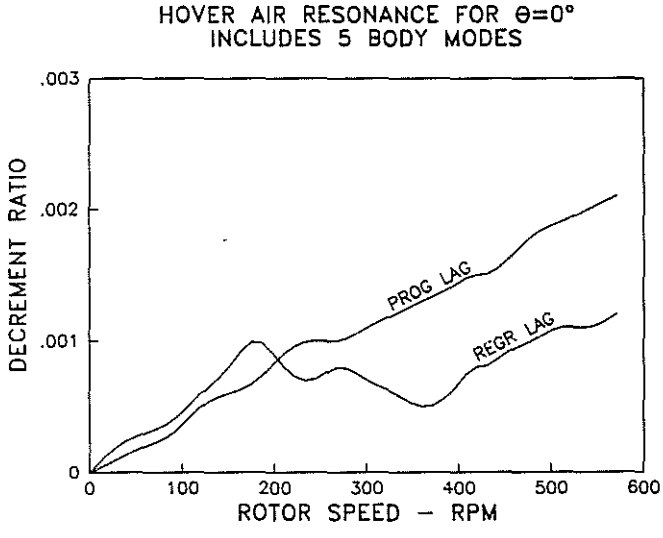

FIG. 14a LAG MODES DAMPING

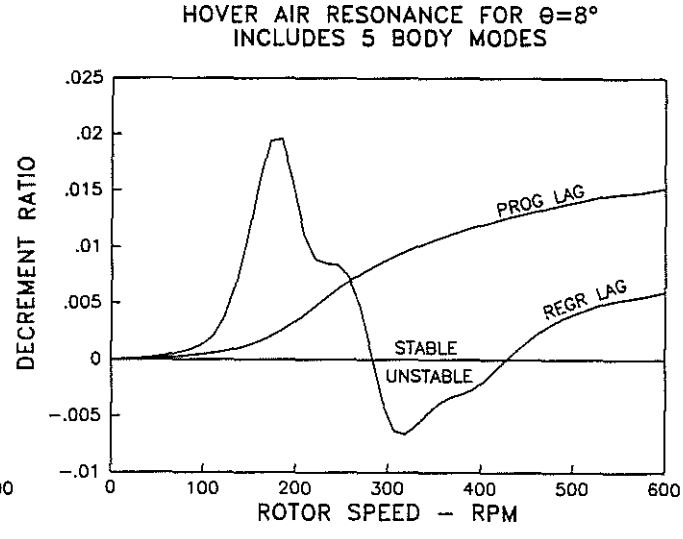

FIG. 14b LAG MODES DAMPING

Figure 15a and 15b examine the number of body modes that is necessary to capture the correct regressing lag mode damping value. For 0° collective pitch, using body pitch degree of freedom only, or pitch and roll only, the predicted lag damping is almost as good as using 5 body DOF. At higher collective pitch, such as 8°, at least pitch and roll body DOFs must be used, otherwise the lag mode instability would not be fully captured.

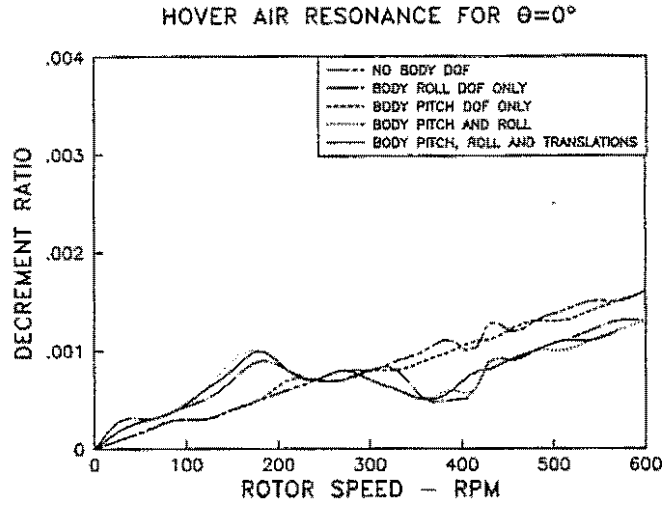

FIG. 15a EFFECT OF BODY MODES ON REGRESSING LAG MODE DAMPING

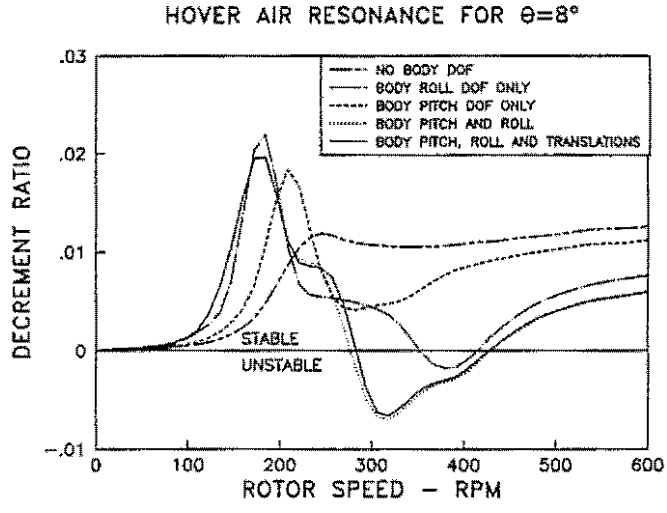

FIG. 15b EFFECT OF BODY MODES ON REGRESSING LAG MODE DAMPING

4.3 Forward Flight Air Resonance

For air resonance study of hingeless rotors in forward flight, a soft-inplane baseline configuration is selected. For this configuration, the precone, pretwist, and blade tip sweep angles are all assumed to be zero. The structural damping for the blade and body modes are neglected. The baseline configuration properties are same as used for hover air resonance stability. For the stability calculations, six coupled modes for each blade (3 flap, 2 lag, 1 torsion), five rigid body modes (longitudinal, lateral, vertical, pitch, roll), and three dynamic inflow components ($\lambda_0, \lambda_{1c}, \lambda_{1s}$) are used. These result in a total of 61 states: 48 states due to rotor (progressing, regressing, coning, differential), 10 states due to body, and 3 states due to inflow. The solution gives 61 complex eigenvalues.

Dynamic Inflow effect

Figure 16 presents the effect of dynamic inflow on blade dampings. Dynamic inflow which introduces unsteady aerodynamic effects has a considerable influence on flap motion. It shows that dynamic inflow reduces the flap mode damping.

Thrust Level Effect

Figure 17 compares the effect of thrust level on regressing lag mode stability. In hovering condition ($\mu = 0$), an increase in thrust level is stabilizing. However, an increase in thrust is destabilizing at low speed. At higher advance ratio, the $C_T/\sigma = .14$ case is more stable than the baseline configuration. While increasing the C_T/σ to .21 is destabilizing. A higher thrust level results in more aerodynamic forces, larger steady deflections (in particular flap) and larger structural couplings.

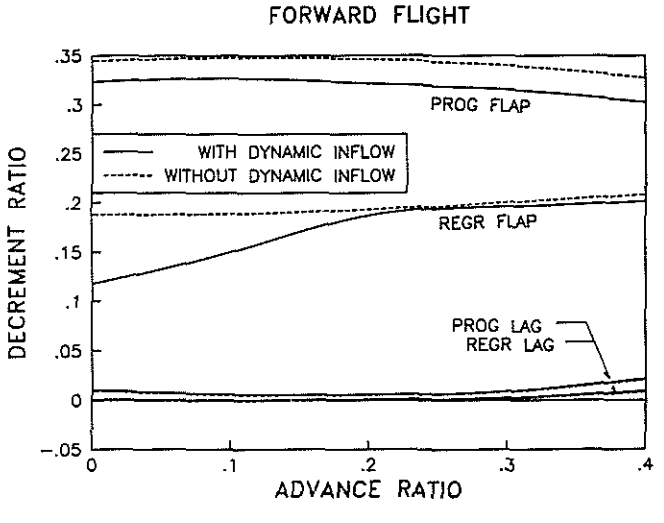

FIG. 16 EFFECT OF DYNAMIC INFLOW ON DAMPINGS IN FORWARD FLIGHT: C_T/σ=.07

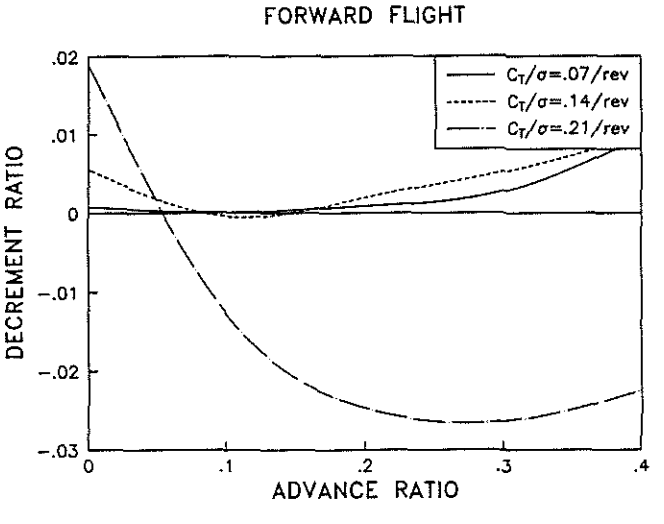

FIG. 17 EFFECT OF THRUST LEVEL ON LAG DAMPING IN FORWARD FLIGHT: C_T/σ=.07

Precone Effect

Figure 18 presents the effect of precone (positive precone is up). Precone influences stability through a steady flap deflection which couples flap and lag motions through coriolis force. The result shows that negative precone is stabilizing, whereas, positive precone is destabilizing for the complete range of forward speed.

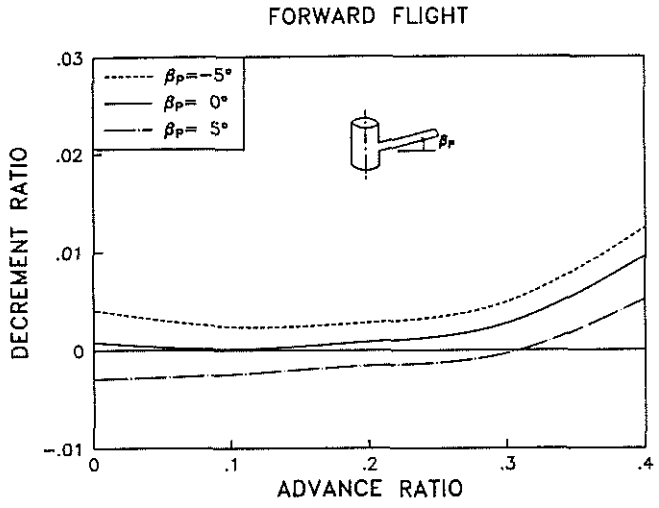

FIG. 18 EFFECT OF PRECONE ON LAG DAMPING IN FORWARD FLIGHT: C_T/σ=.07

Sweep Effect

Figure 19 demonstrates the effect of blade tip sweep on the regressing lag mode stability. The blade tip is swept at the 85% radius location. Positive sweep represents swept back condition (opposite to rotation). The effects of blade sweep are introduced properly in the analysis such that the compatibility conditions of the displacements and slopes are satisfied for moderate rotations in the assembly of two adjoining elements. The sweep introduces pitch-flap coupling. The result shows that sweep backward is beneficial, and forward sweep is destabilizing.

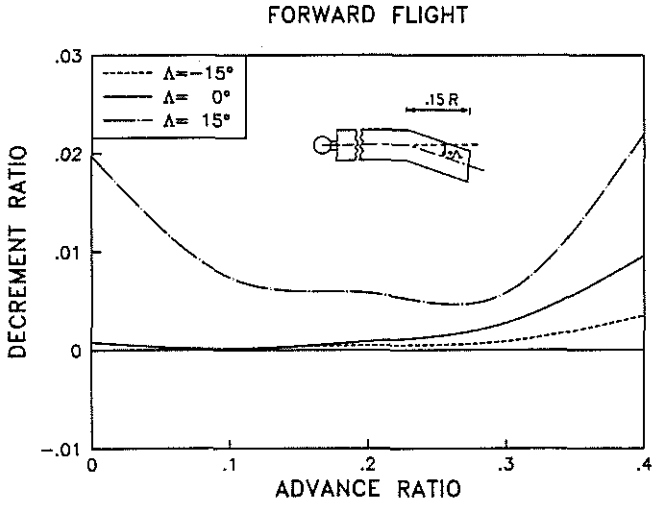

FIG. 19 EFFECT OF SWEEP ON LAG DAMPING IN FORWARD FLIGHT: C_T/σ=.07

Chordwise Stiffness Effect

Figure 20 shows a reduction in chordwise stiffness decreases the regressing lag mode damping. The matched stiffness condition (nonrotating flap and lag frequencies equal) is not helpful. An increase of chordwise stiffness to level of a stiff-inplane rotor has a substantial positive influence on the lag mode stability.

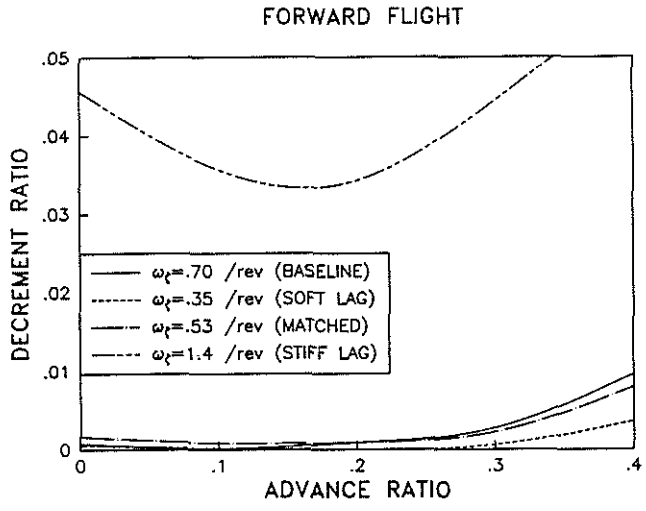

FIG. 20 EFFECT OF CHORDWISE STIFFNESS ON LAG DAMPING IN FORWARD FLIGHT: C_T/σ=.07

Flapwise Stiffness Effect

Air resonance stability is associated with low frequency cyclic flap and lag modes, and the body modes. A decrease in flapwise stiffness reduces the flap frequency and weakens the coupling between the regressing flap, and body, and lag modes, and therefore increases the lag mode stability. Figure 21 presents the effect of structural stiffness in the flapwise direction on the regressing lag mode stability. The beneficial effect of reducing the flapwise stiffness diminishes at higher forward speeds.

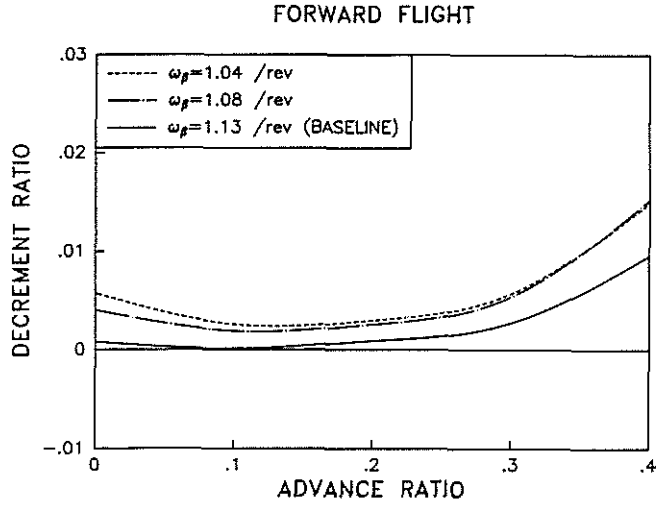

FIG. 21 EFFECT OF FLAPWISE STIFFNESS ON LAG DAMPING IN FORWARD FLIGHT: C_T/σ=.07

Torsional Stiffness Effect

As torsional stiffness is reduced, favorable pitch-lag coupling is increased. Figure 22 indicates that regressing lag mode become more stable with reduced torsional stiffness.

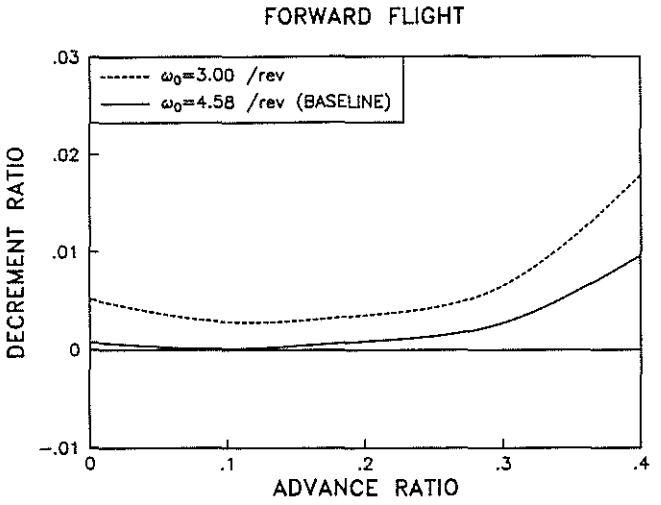

FIG. 22 EFFECT OF TORSIONAL STIFFNESS ON LAG DAMPING IN FORWARD FLIGHT: C_T/σ=.07

Body Inertia Effect

Figures 23 and 24 respectively illustrate the effect of body pitch and roll inertia on the regressing lag mode stability. Since air resonance occurs due to the coalescence of a regressing flap, lag modes and body modes, therefore, the body inertia plays an important role in the coupling of rigid body modes and the low frequency cyclic blade modes. As expected, an increase in body pitch or roll inertia is stabilizing. Roll inertia has a more powerful influence on the lag mode stability than pitch inertia.

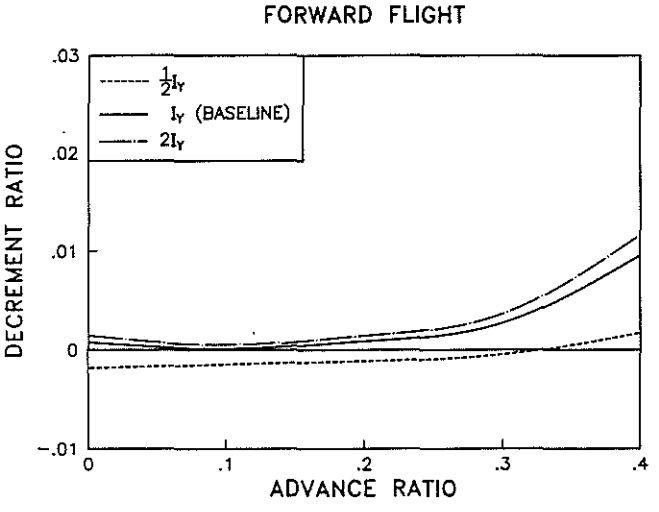

FIG. 23 EFFECT OF PITCH INERTIA ON LAG DAMPING IN FORWARD FLIGHT: C_T/σ=.07

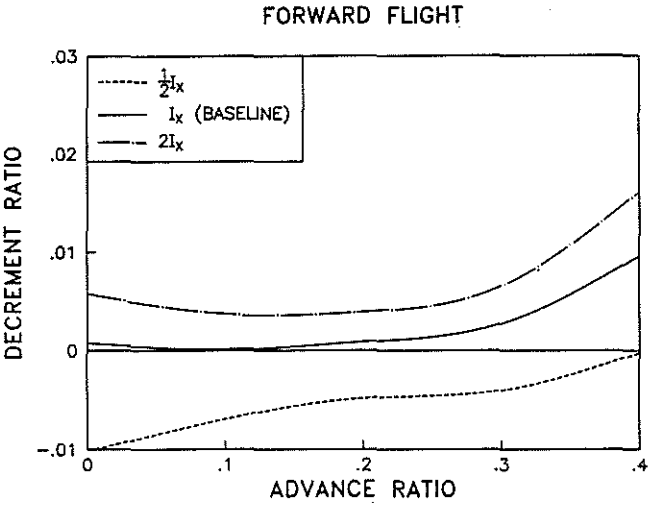

FIG. 24 EFFECT OF ROLL INERTIA ON LAG DAMPING IN FORWARD FLIGHT: C_T/σ=.07

5 CONCLUSION

Base on an air resonance analysis in forward flight using refined structural modeling, coupled trim analysis and dynamic inflow, the following conclusions can be drawn from this investigation.

1. A good correlation of analytical results with experimental data is achieved for ground resonance. The inclusion of dynamic inflow modeling improves the prediction of ground resonance instability.
2. A soft instability occurs at high collective pitch in hover due to coupling of the regressing flap and lag modes with the body modes.
3. For modeling of air resonance stability of a hingeless rotor, pitch and roll rigid body airframe modes must be included.
4. Dynamic inflow modeling increases the regressing lag mode stability slightly in forward flight.
5. Backward sweep of the blade tip stabilizes the lag mode stability.
6. A negative precone is stabilizing in forward flight.
7. A decrease in flapwise stiffness or an increase in chordwise stiffness is stabilizing.
8. Reducing the torsional stiffness raises the lag mode stability.
9. Body inertia plays an important role on stability. Rotor-body aeromechanical stability is more sensitive to roll inertia than to pitch inertia.

Acknowledgements

The authors acknowledge the University of Maryland Computer Center for the computer time. This research work was supported by the Army Research Office, Contract No. DAAL-03-88-C-0002; Technical Monitor, Dr. Robert Singleton.

References

[1] Johnson, W., "Recent Developments in the Dynamics of Advanced Rotor Systems," NASA TM–96669, March 1985.

[2] Ormiston, R. A., "Investigations of Hingeless Rotor Stability," Vertica, Vol. 7, No. 2, 1983, pp. 143–181.

[3] Friedmann, P. P., "Recent Trends in Rotary Wing Aeroelasticity," Vertica, Vol. 11, No. 1/2, 1987, pp. 139–170.

[4] Lytwin, R. T. and Miao, W., "Airborne and Ground Resonance of Hingeless Rotors," Journal of the American Helicopter Society, Vol. 16, No. 2, April 1971.

[5] Burkam, J. E. and Miao, W., "Exploration of Aeroelastic Stability Boundaries with a Soft In–Plane Hingeless Rotor Model," Journal of the American Helicopter Society, Vol. 17, No. 4, Oct. 1972.

[6] Miao, W. and Huber, H. B., "Rotor Aeroelastic Stability Coupled with Helicopter Body Motion," AHS/NASA–Ames Specialists' Meeting on Rotorcraft Dynamics, NASA SP–352, 1974, PP. 137–146.

[7] Ormiston, R. A., "Aeromechanical Stability of Soft Inplane Hingeless Rotor Helicopters," Third European Rotorcraft and Powered Lift Aircraft Forum, Aix–en–Provence, France, Paper No. 25, Sep. 1977.

[8] King,S., "Theoretical and Experimental Investigation into Helicopter Air Resonance," American Helicopter Society Forum, St Louis, Missouri, May, 1983.

[9] Peter,D.A., Gaonkar, G.H., Mitra, A. K., and Reddy, T.S.R., "Sensitivity of Helicopter Aeromechanical Stability to Dynamic Inflow," Vertica, Vol. 6, 1982, pp.59–75.

[10] Johnson, W., "Influence of Unsteady Aerodynamics on Hingeless Rotor Ground Resonance," Journal of Aircraft, Vol. 19, No. 8, Aug. 1982, pp. 668–673.

[11] Friedmann, P. P. and Venkatesan, C., "Influence of Various Unsteady Aerodynamic Models on the Aeromechanical Stability of a Helicopter in Ground Resonance," Second Decennial Specialists' Meeting on Rotorcraft Dynamics, NASA Research Center, Moffett Field, Calif., Nov. 1984.

[12] Bousman, W. G., "An Experimental Investigation of the Effects of Aeroelastic Couplings on Aeromechanical Stability of a Hingeless Rotor Helicopter," Journal of the American Helicopter Society, Vol. 26, No. 1, Jan. 1981.

[13] Bousman, W. G., "A comparison of Theory and Experiment for Coupled Rotor–Body Stability of a Hingeless Rotor Model in Hover," Presented at the Integrated Technology Rotor(ITR) Methodology Assessment Workshop, NASA Ames Research Center, Moffett Field, Calif., June 1983.

[14] Jang, J. and Chopra, I., "Ground and Air Resonance of Bearingless Rotors in Hover," AIAA Dynamics Specialist Conference, Monterey, Calif., April 1987.

[15] Dull, A. L., "Aeroelastic Stability of Bearingless Rotors in Forward Flight," American Helicopter Society 43rd Annual Forum, St Louis, Missouri, May 1987.

[16] Jang, J. and Chopra, I., "Air Resonance of an Advanced Bearingless Rotor in Forward Flight," Second International Rotorcraft Basic Research Conference, College Park, Maryland, Feb. 1988.

[17] Friedmann, P. P., and Venkatesan C., "Coupled Helicopter Rotor/Body Aeromechanical Stability Comparison of Theoretical and Experimental Results," Journal of Aircraft, Vol. 22, No. 2, Feb. 1985, PP 148-155.

[18] Hodges, D. H. and Dowell, E. H., "Nonlinear Equations of Motion for the Elastic Bending and Torsion of Twisted Nonuniform Rotor Blades," NASA TN–D 7818, Dec. 1974.

[19] Pitt, D. M. and Peters, D. A., "Theoretical Prediction of Dynamic Inflow Derivatives," Vertica, Vol. 5, No. 1, 1981, pp. 21–34.

[20] Panda, B., "Technical Note: Assembly of Moderate–Rotation Finite Elements Used in Helicopter Rotor Dynamics," Journal of the American Helicopter Society, Vol. 32, No. 4, Oct. 1987.

[21] Panda, B. and Chopra, I., "Dynamics of Composite Rotor Blades in Forward Flight with Application of Finite Element in Time," Tenth Anniversary of Vertica, Special Issue, 1986.

[22] Panda, B. and Chopra, I., "Flap-Lag-Torsion Stability in Forward Flight," Journal of the American Helicopter Society, Vol. 31, No. 2, April 1986.

[23] Lim,J.W., and Chopra,I., "Stability Sensitivity Analysis for the Aeroelastic Optimization of a Helicopter Rotor," The AIAA SDM Conference, Williamsburg, VA, April 1988.

[24] Sivaneri, N. T. and Chopra, I., "Finite Element Analysis for Bearingless Rotor Blade Aeroelasticity," Journal of the American Helicopter Society, Vol. 29, No. 2 April 1984, pp.42-51.